7. FRACTURE

Fracture can be defined as the process of separation (or fragmentation) of a solid into two or more parts under the action of a stress. So-defined, fracture can certainly be identified as one type of engineering failure in which a design can no longer perform its intended function. Ductile fracture is accompanied by gross deformation and shear fracture due to slip (sometimes described as "graceful failure" due to the resulting nonlinear load-displacement curve). Brittle fracture occurs with no gross deformation and often is accompanied by rapid crack propagation and catastrophic failure. Brittle fracture is not confined to materials normally thought of as brittle but can occur in ductile materials at high strain rates (impact), at low temperatures, at the root of notches, and in the presence of cracks.

The presence of cracks may weaken the material such that fracture occurs at stresses much less than the yield or ultimate strengths (see Fig. 7.1). Fracture mechanics is the methodology used to aid in selecting materials and designing components to minimize the possibility of fracture from cracks.

In understanding the effect of brittle fracture in performance of engineering designs, it is useful to first examine the strength potential of engineering materials. Consider the force (or stress)-displacement relationship between two atoms as shown in Fig. 7.2. If this relation is modeled as a sine wave then the equation can be written as:

$$\sigma = \sigma_{max} \sin\pi\left(\frac{x}{\lambda/2}\right) \tag{7.1}$$

where σ_{max} is the maximum stress on the curve, x is the displacement and $\lambda/2$ is the half wave length of the sine wave. Applying uniaxial Hooke's law ($\sigma = E\varepsilon$) where $\varepsilon = \left(\frac{x - x_e}{x_e}\right)$ and small angle approximations ($\sin\theta = \theta$) of Eq. 7.1 gives

$$\sigma = E\varepsilon = E\left(\frac{x - x_e}{x_e}\right) = \sigma_{max}\left(\frac{\pi x}{\lambda/2}\right) \tag{7.2}$$

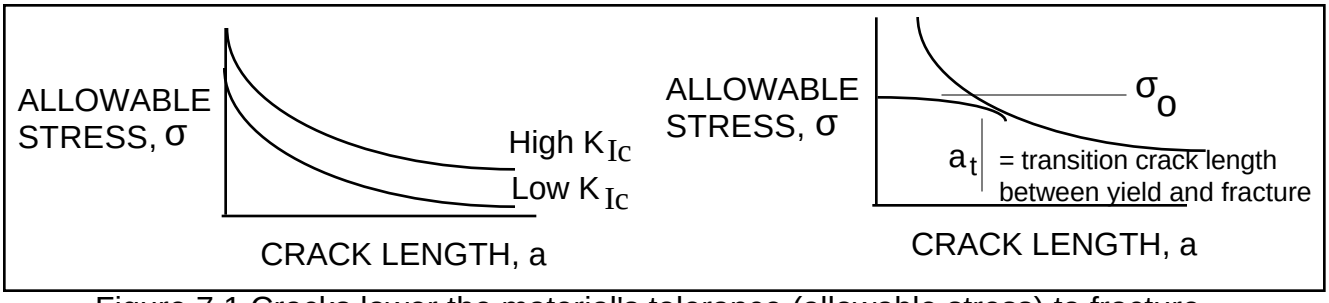

Figure 7.1 Cracks lower the material's tolerance (allowable stress) to fracture.

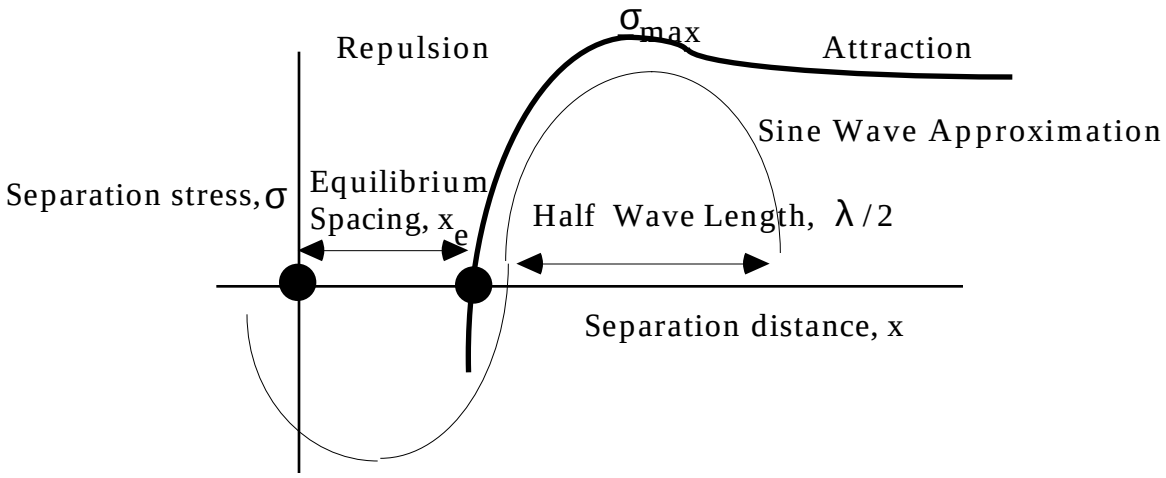

Figure 7.2 Attractive/repulsive force-distance curve between two atoms

where E is the elastic modulus and x_e is the equilibrium distance (a.k.a., lattice spacing) between the atoms. Assuming $\lambda/2 = x_e$ and solving Eq. 7.2 for σ_{max} gives.

$$\sigma_{max} = \frac{E}{\pi}\sqrt{\frac{\gamma_s}{x_e}} \tag{7.3}$$

where σ_{max} is the maximum cohesive strength (i.e., greatest strength potential) of a material.

Another approach is to evaluate the work done in pulling the atoms apart:

$$W = \int_o^x F(x)dx = \int_o^x \sigma(x)Adx = \int_o^{\lambda/2} \sigma_{max} \sin\frac{\pi x}{\lambda/2} Adx \tag{7.4}$$

Solving the integral for the work per unit area (W/A) and setting this equal to the resisting energy to create new fracture surfaces gives:

$$\frac{W}{A} = \sigma_{max}\frac{\lambda}{\pi} = 2\gamma_s \tag{7.5}$$

where γ_s is the fracture surface energy. Solving Eq. 7.5 for λ results in $\lambda = \frac{2\gamma_s\pi}{\sigma_{max}}$. Substituting this expression for λ into Eq. 7.2 and solving for σ_{max}

$$\sigma_{max} = \sqrt{\frac{E\gamma_s}{x_e}} \tag{7.6}$$

To check how well expressions in Eq. 7.3 and 7.6 compare to actual strengths of materials, steel is used as an example where E = 200 GPa, γ_s = 1 J/m^2, and $x_e = a_o = 2.5\text{x}10^{-10}$ m. In this case, Eq. 7.3 gives σ_{max} = 63.7 GPa and Eq. 7.6 gives σ_{max} = 28.3 GPa. Since most steels have ultimate strengths in the 0.5 to 1 GPa range, something

in real materials must be preventing them from reaching the strength potential predicted by the maximum cohesive strength.

In engineering design, stress raisers such as holes can raise the local stress to levels much greater than the remote or applied stress. For example, for a plate with a hole in it subjected to uniaxial, uniform tensile stress (see Fig. 7.3) the elasticity solutions in polar coordinates with variables r and θ are:

$$\sigma_{rr} = \frac{\sigma}{2}\left[\left(1-\frac{R^2}{r^2}\right)+\left(1+\frac{3R^2}{r^2}-1\right)\cos 2\theta\right]$$
$$\sigma_{\theta\theta} = \frac{\sigma}{2}\left[\left(1+\frac{R^2}{r^2}\right)+\left(1+\frac{3R^2}{r^2}\right)\cos 2\theta\right] \qquad (7.7)$$

At the edge of the hole for θ=0°, Eqs. 7.7 can be rewritten in Cartesian coordinates as:

$$\sigma_{xx} = \sigma_{rr} = \frac{\sigma}{2}\left[\left(1-\frac{R^2}{r^2}\right)-\frac{3R^2}{r^2}\right]$$
$$\sigma_{yy} = \sigma_{\theta\theta} = \frac{\sigma}{2}\left[2+\frac{R^2}{r^2}+\frac{3R^2}{r^2}\right] \qquad (7.8)$$

Finally at the edge of the hole, where r=R, the stresses are:

$$\sigma_{xx} = \sigma_{rr} = 0$$
$$\sigma_{yy} = \sigma_{\theta\theta} = 3\sigma \qquad (7.9)$$

The stress concentration factor can be defined as $k_t = \frac{\sigma_{local}}{\sigma_{remote}}$. For the stress in the y-direction, k_t is 3. Thus, the local stress at the edge of the hole is three times the remotely applied stress regardless of the size of the hole as long as the hole diameter is small relative to the width of the place.

In the case of an elliptical hole in uniaxial, uniform tension (see Fig. 7.3), the stress in the y-direction can be related to the major and minor axes such that:

$$\sigma_{yy} = \sigma\left(1+2\frac{c}{a}\right) = \sigma\left(1+2\sqrt{\frac{c}{\rho}}\right) \qquad (7.10)$$

where the radius of the ellipse tip is $\rho = \frac{a^2}{c}$. The stress concentration factor for the elliptical hole is no longer constant as it is for the circular hole but is a function of the ellipse geometry:

$$k_t = \left(1+2\sqrt{\frac{c}{\rho}}\right) \approx \left(2\sqrt{\frac{c}{\rho}}\right) \qquad (7.11).$$

Note in this case that as the minor axis 2a shrinks to zero (e.g., as in a crack), ρ goes to zero and the stress concentration factor in Eq. 7.11 goes to infinity.

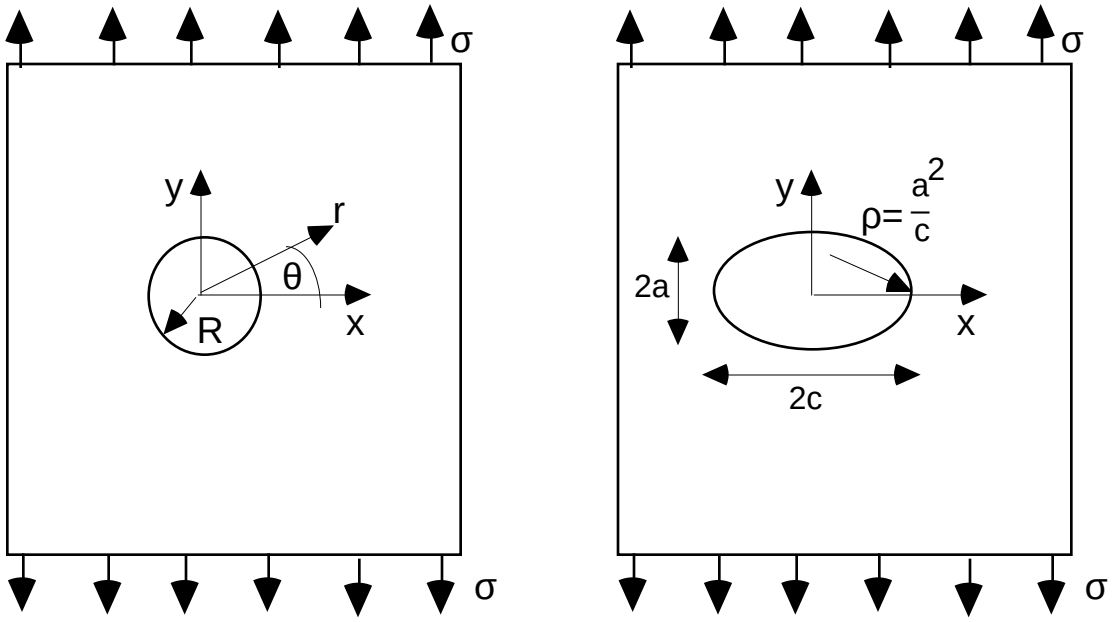

Figure 7.3 Plates with circular and elliptical holes, subjected to uniform tensile stresses

Thus, elliptically-shaped features can have local stresses which are much greater than remote stresses. If these local stresses approach the maximum cohesive strength on a microscopic scale, then failure can initiate at such features ultimately leading to failure of the material.

However, stress analyses such as these do not lend themselves to application in engineering because infinite stress concentration factors are not usable in design. Therefore, E. Orowan proposed the following approach:

a) assume cracks exist

b) assume these cracks are elliptically shaped with the appropriate stress solution

c) assume at fracture that the theoretical cohesive strength, σ_{max}, is exceeded by the stress, σ_{yy}, at the tip of the ellipse.

Combining Eqs. 7.10 and 7.6 (simplifying per Eq. 7.11) gives:

$$\sigma_{\max} = \sigma_{yy} \qquad \sqrt{\frac{E\gamma_s}{a_o}} = \sigma \left(2\sqrt{\frac{c}{\rho}}\right) \tag{7.12}$$

If fracture occurs at an atomistically-sharp ellipse tip, then let $\rho \approx a_o$ and the remote stress required to cause brittle fracture is:

$$\sigma_f = \sqrt{\frac{E\gamma_s}{4c}} \tag{7.13}$$

A. A. Griffith proposed a different solution by assuming neither a crack shape or a stress solution. Instead, Griffith stated that the criterion for brittle fracture is:

"A crack will propagate when the decrease in elastic strain energy is as least equal to the energy required to create new crack surfaces."

The starting point for Griffith's solution is to evaluate the strain energy in the volume surrounding the area in a plate (see Fig. 7.4) of thickness, t, and width, >>>W≈∞, under uniform uniaxial tension, σ, into which a crack could be introduced. For a crack of length, 2c, the stored elastic strain energy is:

$$U_E = \frac{1}{2}\sigma\varepsilon V = \frac{\sigma^2}{2E}\left(\pi c^2 t\right) \approx \frac{\sigma^2}{E}\left(\pi c^2 t\right) \qquad (7.14)$$

The resistance to fracture is related to the energy required to create new fracture surfaces, U_S, which is a function of the fracture surface energy, γ_S, and the surface area of the crack, A=2 (2ct), such that:

$$U_s = \gamma_s A = \gamma_s(2(2ct)) = \gamma_s(4ct) \qquad (7.15)$$

The change in stored energy from the uncracked panel to the cracked panel is:

$$\Delta U = U_s - U_E = \gamma_s A = \gamma_s(4ct) - \frac{\sigma^2}{E}\left(\pi c^2 t\right) \qquad (17.16)$$

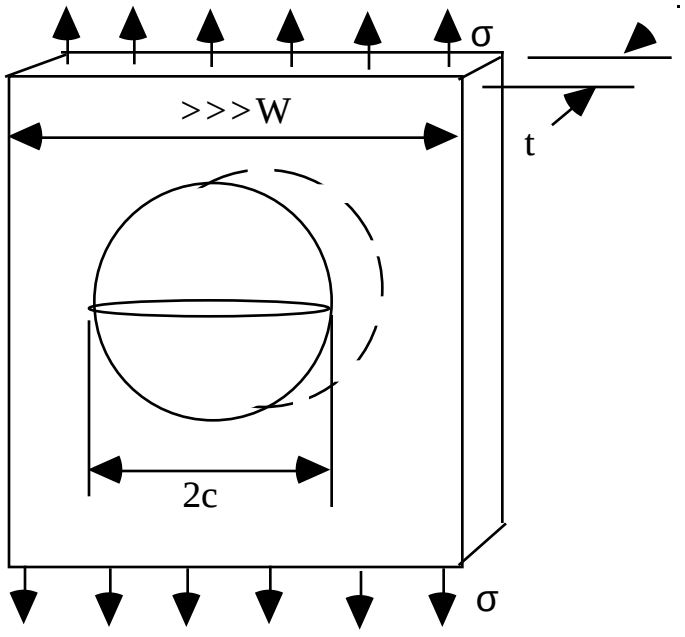

Figure 7.4 Uniformly stress plate of thickness, t, and width, W, into which a crack of length, 2c, will be introduced.

The three energy terms, U_S, U_E and ΔU, are plotted as functions of half crack length, c, in Fig. 7.5. It is apparent that the critical condition for unstable, brittle fracture is reached when $c=c_c$ and $\frac{d\Delta U}{dc}=0$ at the peak of the ΔU curve. Differentiating Eq. 17.6, setting it equal to zero, and solving for the stress at which brittle fracture occurs results in the following:

$$\text{Plane stress } (\sigma_z = 0) \quad \sigma_f = \sqrt{\frac{2\gamma_s E}{\pi c}}$$

$$\text{Plane strain } (\varepsilon_z = 0) \quad \sigma_f = \sqrt{\frac{2\gamma_s E}{(1-\nu^2)\pi c}} \qquad (17.17)$$

It is interesting to compare Eqs. 17.13 and 17.17 and note that they only differ by factors of 1/4 and $2/\pi$ under the radical, respectively. However, from a physical standpoint Eq 17.17 is more "satisfying" because it is based purely on an energy balance, making no assumptions about crack shapes or stress solutions.

Although Eq. 17.17 gives a physical relation for the critical fracture stress, it has little engineering application because it is specific to the case of uniform stress and infinite relative dimensions. G. Irwin attempted to place an engineering sense on the understanding of crack/structure/material interactions. The resulting discipline is known as Fracture Mechanics, and when dealing with non plastic situations, Linear Elastic Fracture Mechanics (LEFM).

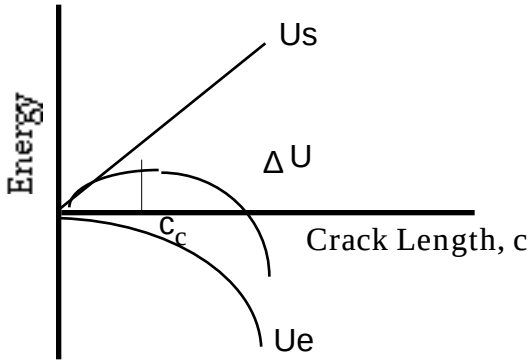

Figure 7.5 Graphical representation of the Griffith energy balance

Irwin used the Griffith approach as the basis for his subsequent development, first denoting a new engineering term, G, as the strain energy release rate and crack driving force:

$$G = \frac{dU}{dA} \approx \frac{dU}{tda} \tag{7.18}$$

where U is the potential energy of the cracked panel, a is now defined as the half crack length (note, a=c), and t is the plate thickness. In this context, $G \approx 2\gamma_s$ such that the Griffith relation for fracture stress is written in LEFM as:

$$\sigma_f = \sqrt{\frac{GE}{\pi a}} \tag{7.19}$$

The utility of G for engineering purposes can be illustrated by an example of a center cracked panel subjected to a uniform, uniaxial tensile stress (see Fig. 7.6). In this case, it can be shown that:

$$\begin{aligned} &\text{Fixed load} && G = \frac{1}{2} P^2 \left(\frac{dC}{da}\right) && \text{for t = 1} \\ &\text{Fixed displacement} && G = -\frac{1}{2} P^2 \left(\frac{dC}{da}\right) && \text{for t = 1} \end{aligned} \tag{7.20}$$

where $\frac{dC}{da}$ is the compliance change (compliance is $C = \frac{\delta}{P}$) with crack extension, da, P is the applied load, and δ is the displacement. For a known geometry, the dimensionless compliance, EBC (E is elastic modulus and B=t is the specimen thickness) is plotted versus dimensionless crack length, a/W (W is the specimen width). At the critical condition when the plate fractures, P=P_c and the dimensionless compliance is $EBC_c = EB\frac{\delta_c}{P_c}$ (see Fig. 7.6) From the master compliance curve for the particular geometry, $\frac{dC_c}{da_c}$ is determined and the critical G at fracture is:

$$G_c = \frac{1}{2} P_c^2 \left(\frac{dC_c}{da_c}\right) \tag{7.21}$$

Although Eq. 7.21 gives a readily accessible engineering quantity for critical fracture, it still lacks utility for general applicability to engineering design. An alternative approach is to look at the stress at the crack tip. The near field stresses for a through crack in an infinite plate, subjected to a uniform, uniaxial tensile stress are (see Fig. 7.7):

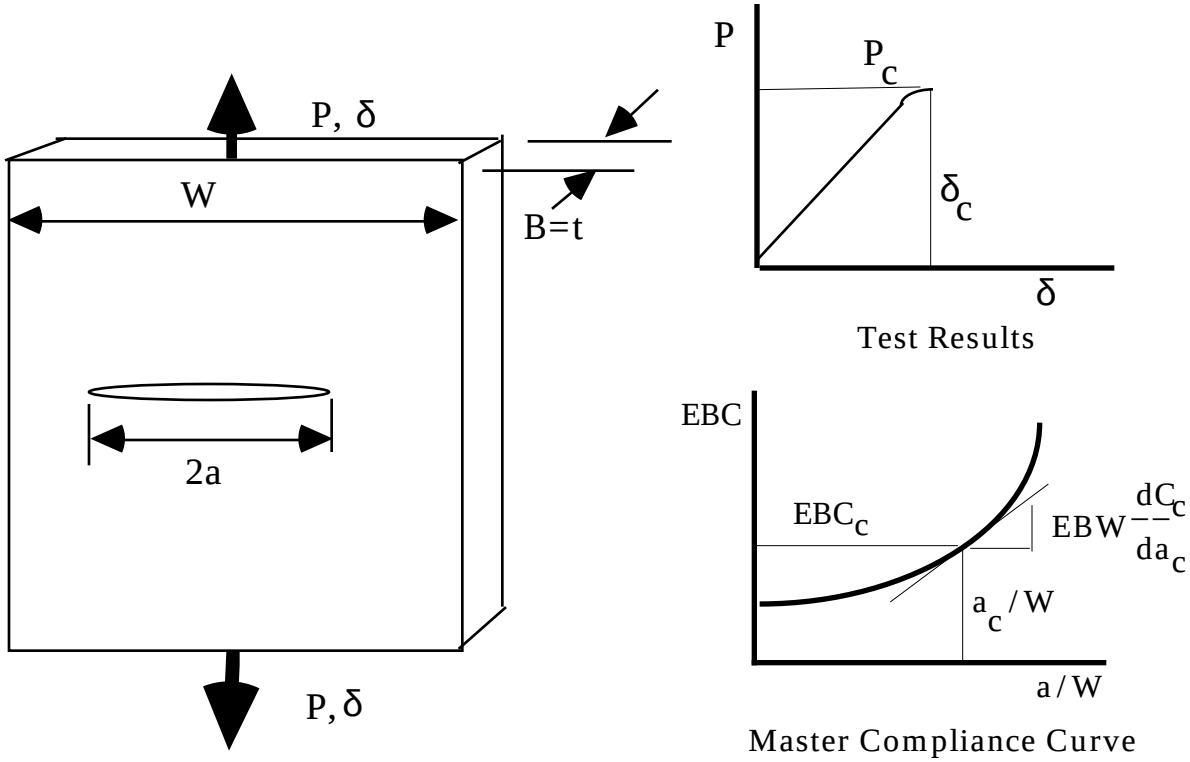

Figure 7.6 Illustration of method for determining critical strain energy release rate

$$\sigma_{xx} = \sigma\frac{a}{\sqrt{2r}}\cos\frac{\theta}{2}\left[1-\sin\frac{\theta}{2}\sin\frac{3\theta}{2}\right]+.....$$

$$\sigma_{yy} = \sigma\frac{a}{\sqrt{2r}}\cos\frac{\theta}{2}\left[1+\sin\frac{\theta}{2}\sin\frac{3\theta}{2}\right]+.....$$

$$\sigma_{xy} = \tau_{xy} = \sigma\frac{a}{\sqrt{2r}}\cos\frac{\theta}{2}\sin\frac{\theta}{2}\cos\frac{3\theta}{2}+.....$$

(7.22)

$\sigma_{zz} = 0$ and $\tau_{yz} = \tau_{zx} = 0$ for plane stress

or

$\sigma_{zz} = \nu(\sigma_{xx} + \sigma_{yy})$ for plane strain

Note in Eqs. 7.22 that as $r \to 0$, the stresses predicted by the equations, all become infinite, thus rendering the equations unusable for calculating the critical stress at the crack tip for engineering design purposes. Irwin, however, took a different approach and defined a stress intensity factor, K, which could uniquely define the stress state at the crack tip, without the need to determine the actual stress such that:

$$K = \sigma\sqrt{\pi a} \qquad (7.23)$$

The units of K are a bit unusual as $MPa\sqrt{m}$.

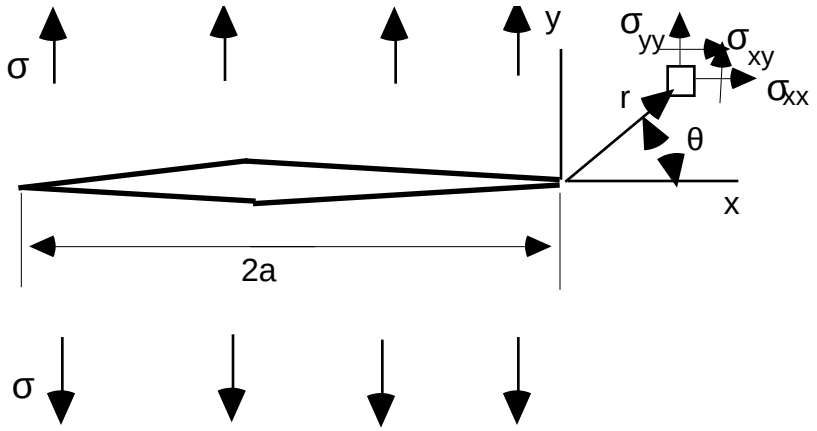

Figure 7.7 Near field stress state for a crack in an infinite plate subjected to uniform, uniaxial tension.

Irwind did not chose the epression for K arbitrarily. Note that K and G are related:

$$\text{If } \sigma_f = \sqrt{\frac{GE}{\pi a}} \text{ then } \sigma^2 = \frac{GE}{\pi a} \text{ and } G = \frac{\sigma^2 \pi a}{E}$$
$$\text{But, since } K = \sigma\sqrt{\pi a} \text{ then } G = \frac{K^2}{E} \qquad (7.24)$$

Now Eq. 7.22 can be written in terms of K:

$$\sigma_{xx} = \sigma \frac{K}{\sqrt{2\pi r}} \cos\frac{\theta}{2}\left[1-\sin\frac{\theta}{2}\sin\frac{3\theta}{2}\right]+.....$$
$$\sigma_{yy} = \sigma \frac{K}{\sqrt{2\pi r}} \cos\frac{\theta}{2}\left[1+\sin\frac{\theta}{2}\sin\frac{3\theta}{2}\right]+.....$$
$$\sigma_{xy} = \tau_{xy} = \sigma \frac{K}{\sqrt{2\pi r}} \cos\frac{\theta}{2}\sin\frac{\theta}{2}\cos\frac{3\theta}{2}+.....$$
$$\sigma_{zz} = 0 \text{ and } \tau_{yz} = \tau_{zx} = 0 \text{ for plane stress} \qquad (7.25)$$
or
$$\sigma_{zz} = \nu(\sigma_{xx} + \sigma_{yy}) \text{ for plane strain}$$

Again, note that although Eqs. 7.25 still predict infinite stresses at the crack tip, the stress intensity factor can now be used to define the stress <u>state</u> at the crack tip. From an engineering standpoint, the stress intensity factor can be used like stress to predict the critical condition at fracture:

$$\text{Fracture OCCURS if FS} \le 1 \text{ where} \quad \text{FS} = \frac{K_c}{K} \qquad (7.26)$$

where Kc is a material property known as fracture toughness and K is the stress intensity factor at a particular combination of crack length and stress in the component. Several things are important in Eq. 7.26.

The first is related to the "mode" of the fracture or loading. There are three modes designated via Roman numerals as: I (opening), II (sliding) and III (tearing) as illustrated in Fig. 7.8. Note that the most critical mode is Mode I because the crack tip carries all the stress whereas in Modes II and III some of the stress is carried by interaction of the opposing crack faces.

A second point is that the stress intensity factor defined in Eq. 7.23 is for the special case of idealized crack in an infinite plate. Real cracks are affected by the geometry of the component, the applied stress field, and other factors. Thus, Eq. 7.23 can be generalized as

$$K = Y\sigma\sqrt{\pi a} = \alpha\sigma\sqrt{\pi a} = F\sigma\sqrt{\pi a} \qquad (7.27)$$

where Y, F and a are geometrical correction factors which maintain the uniqueness of the stress intensity factor by accounting for the particular geometry. For example, a center through crack in a plate of finite width W, has a Y of ~1.12. In other words, the stress intensity factor is about 12% greater in a finite width plate than for an infinitely wide plate. Geometrical correction factors are found from closed form solutions, finite element analyses, and experimental methods such as photoelastcity. Many handbooks of stress intensity factors for common and not so common geometries have been complied. Some common geometries are shown in Fig. 7.9

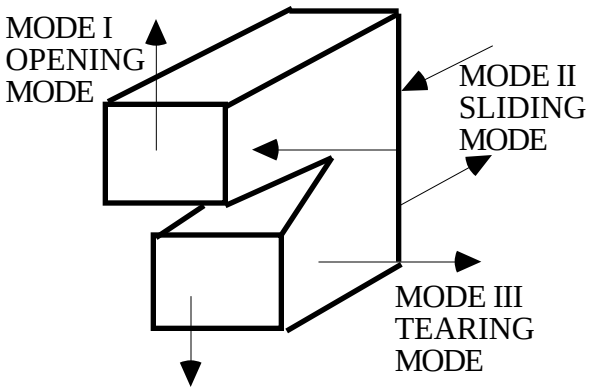

Figure 7.8 Fracture modes

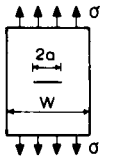

$$K_I = \sigma\sqrt{\pi a}\left(\sec\frac{\pi a}{W}\right)^{\frac{1}{2}}$$

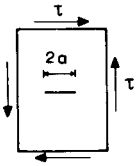

$$K_{II} = \tau\sqrt{\pi a}\left(\text{small } \frac{a}{W}\right)$$

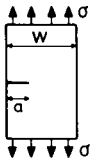

$$K_I = 1.12\,\sigma\sqrt{\pi a}\left(\text{small } \frac{a}{W}\right)$$

or $K_I = Y\sigma\sqrt{a}$

with $Y = 1.99 - 0.41\frac{a}{W} + 18.7\left(\frac{a}{W}\right)^2 - 38.48\left(\frac{a}{W}\right)^3 + 53.85\left(\frac{a}{W}\right)^4$

$(1.99 = 1.12\sqrt{\pi})$

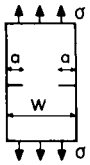

$$K_I = 1.12\,\sigma\sqrt{\pi a}\left(\text{small } \frac{a}{W}\right)$$

or $K_I = Y\sigma\sqrt{a}$

with $Y = 1.99 + 0.76\frac{a}{W} - 8.48\left(\frac{a}{W}\right)^2 + 27.36\left(\frac{a}{W}\right)^3$

$(1.99 = 1.12\sqrt{\pi})$

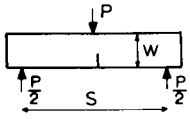

Thickness B

$$K_I = \frac{PS}{BW^{3/2}}\left[2.9\left(\frac{a}{W}\right)^{1/2} - 4.6\left(\frac{a}{W}\right)^{3/2} + 21.8\left(\frac{a}{W}\right)^{5/2} - 37.6\left(\frac{a}{W}\right)^{7/2} + 38.7\left(\frac{a}{W}\right)^{9/2}\right]$$

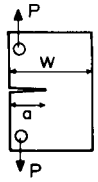

Thickness B

$$K_I = \frac{P}{BW^{1/2}}\left[29.6\left(\frac{a}{W}\right)^{1/2} - 185.5\left(\frac{a}{W}\right)^{3/2} + 655.7\left(\frac{a}{W}\right)^{5/2} - 1017\left(\frac{a}{W}\right)^{7/2} + 63.9\left(\frac{a}{W}\right)^{9/2}\right]$$

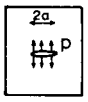

p per unit thickness

$K_I = p\sqrt{\pi a}$

$$K_{I_{max}} = 1.12\frac{\sigma}{\Phi}\sqrt{\pi a}$$

$$K_{I_{min}} = 1.12\frac{\sigma}{\Phi}\sqrt{\pi a^2/c}$$

$$\Phi = \int_0^{\pi/2}\left[1 - \frac{c^2 - a^2}{c^2}\sin^2\varphi\right]d\varphi$$

$$\Phi \approx \frac{3\pi}{8} + \frac{\pi}{8}\frac{a^2}{c^2}$$

Figure 7.9 Common and practical stress intensity factors

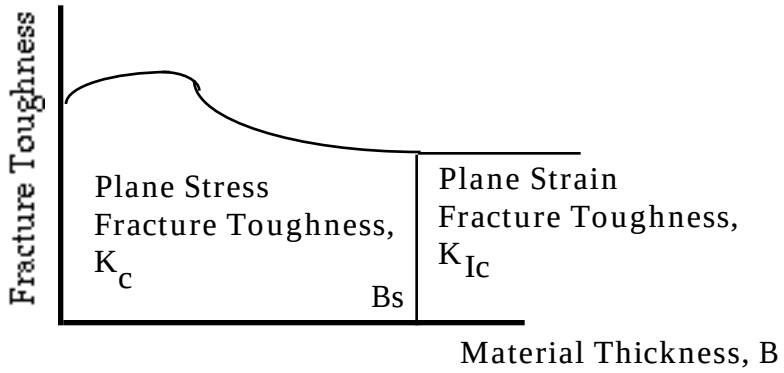

Figure 7.10 Fracture toughness as a function of material thickness.

The third point is that the most critical fracture toughness of the material must be measured so as to be geometry independent. Specifically, the plane stress fracture toughness is a function of material thickness and is an important consideration when determining fracture toughness in sheet material. Plane strain fracture toughness is independent of material thickness and is less than the plane stress fracture toughness as illustrated in Fig. 7.10.

When conducting fracture toughness tests, especially of metals, three critical aspects must be addressed if a valid test is to result. The first is a valid stress intensity factor for the particular geometry being tested. Geometries often used include center cracked panel, three- or four-point flexure and compact tension (see Fig. 7.9). The second is that the dimensions are in proper proportion to assure a valid stress intensity factor and a thick enough specimen for plane strain conditions. ASTM recommends a thickness such that:

$$B \geq 2.5\left(\frac{K_{Ic}}{S_{ys}}\right)^2 \tag{7.28}$$

where S_{YS} is the yield strength of the material and K_{Ic} is the plane strain fracture toughness. Finally, a plasticity requirement must be met where for a valid test:

$$\frac{P_{\max}}{P_Q} \leq 1.1 \tag{7.29}$$

where P_{max} is the maximum load recorded during the fracture test and P_Q is the load at which the load-displacement curve deviates from linearity.

Various trends in fracture toughness are related to material type. For example, as yield point increases, fracture toughness generally decreases since yield points close to the ultimate tensile strength of the material indicate low ductility and tendency to brittle fracture (see Fig. 7.11)

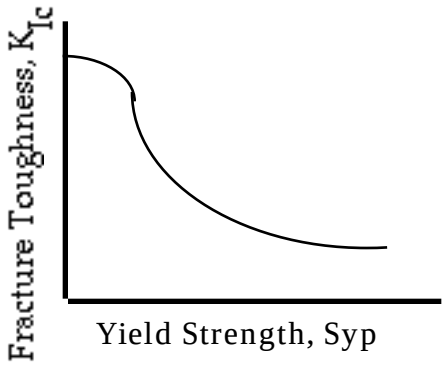

Figure 7.11 General relation between fracture toughness and yield strength

The type of atomic bonding can indicate tendency to brittle fracture (see Fig. 7.12). In general, covalent and ionic bonds as are found in ceramics, glasses and polymers usually leas to lower fracture toughness. Metallic bonds usually lead to higher fracture toughness. Some materials, such as composites, may have relatively high apparent fracture toughness values although the applicability of LEFM to these materials is debatable.

Design philosophies can take several forms, all based on the basic relation that fracture will occur when the stress intensity factor in the component is equal to the fracture toughness of the material such that:

$$\text{Fractures OCCURS if } K_{Ic} = K_I \qquad K_{Ic} = Y\sigma\sqrt{\pi a} \tag{7.30}$$

in which K_{Ic} is a material property

Y is a function of the geometry

σ is a design stress

a is an allowable flaw (crack)

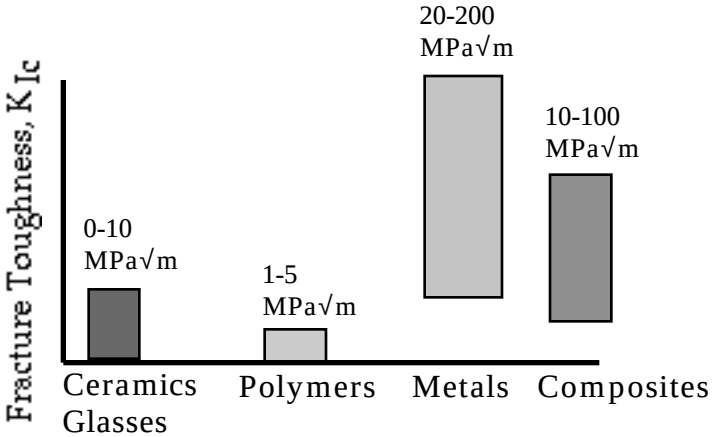

Figure 7.12 Relative comparisons of fracture toughness for various materials

For example, in the design of a nuclear pressure vessel:

a) Material is chosen for certain properties (corrosion resistance, etc.). This fixes K_{Ic}.

b) In the component, allow for the presence of large flaw since these are detectable and correctable. This fixes Y and a_c.

c) Design for the allowable stress, σ, to accommodate K_{Ic}, Y and a_c.

In a different example, an aerospace application:

a) Material is chosen for certain properties (high yield strength, low density, etc). This fixes K_{Ic}.

b) In the component, fix the design stress, σ, for high performance or high payload to weight ratio, etc. This fixes σ.

c) Use nondestructive testing to find a before it reaches critical Y and a_c.

Another example is the clever use of cracks to provide a warning before catastrophic fracture can occur. In the leak before break philosophy, the thickness of a pressure vessel is chosen so that a crack will penetrate the wall before it can reach a critical size to cause brittle fracture. In this way, the presence of the crack can be easily spotted without expensive (and often unreliable) non destructive test methods.